European Polymer Journal 47 (2011) 1569–1577

Contents lists available at ScienceDirect

European Polymer Journal

journal homepage: www.elsevier.com/locate/europolj

Enhanced mechanical performance and biological evaluation of a PLGA coated β-TCP composite scaffold for load-bearing applications

Yunqing Kang [a], Allison Scully [b], Daniel A. Young [a,c], Sungwoo Kim [a], Helen Tsao [a], Milan Sen [d], Yunzhi Yang [a,b,*]

[a] Department of Restorative Dentistry and Biomaterials, The University of Texas Health Science Center at Houston, Houston, TX, USA
[b] Department of Bioengineering, Rice University, Houston, TX, USA
[c] School of Biomedical Engineering and Imaging, The University of Tennessee Health Science Center, Memphis, TN, USA
[d] Department of Orthopedic Surgery, The University of Texas Health Science Center at Houston, Houston, TX, USA

ARTICLE INFO

Article history:
Received 5 October 2010
Received in revised form 3 May 2011
Accepted 7 May 2011
Available online 13 May 2011

Keywords:
Poly(lactic-co-glycolic acid)
β-Tricalcium phosphate
Functional composites
Scaffold
Bone tissue engineering

ABSTRACT

Porous β-tricalcium phosphate (β-TCP) has been used for bone repair and replacement in clinics due to its excellent biocompatibility, osteoconductivity, and biodegradability. However, the application of β-TCP has been limited by its brittleness. Here, we demonstrated that an interconnected porous β-TCP scaffold infiltrated with a thin layer of poly(lactic-co-glycolic acid) (PLGA) polymer showed improved mechanical performance compared to an uncoated β-TCP scaffold while retaining its excellent interconnectivity and biocompatibility. The infiltration of PLGA significantly increased the compressive strength of β-TCP scaffolds from 2.90 to 4.19 MPa, bending strength from 1.46 to 2.41 MPa, and toughness from 0.17 to 1.44 MPa, while retaining an interconnected porous structure with a porosity of 80.65%. These remarkable improvements in the mechanical properties of PLGA-coated β-TCP scaffolds are due to the combination of the systematic coating of struts, interpenetrating structural characteristics, and crack bridging. The *in vitro* biological evaluation demonstrated that rat bone marrow stromal cells (rBMSCs) adhered well, proliferated, and expressed alkaline phosphatase (ALP) activity on both the PLGA-coated β-TCP and the β-TCP. These results suggest a new strategy for fabricating interconnected macroporous scaffolds with significantly enhanced mechanical strength for potential load-bearing bone tissue regeneration.

1. Introduction

Bone grafts are needed for repairing large craniofacial and skeletal defects resulting from congenital malformation, oncologic resection, pathological degenerative bone destruction, and common fractures [1–3]. Current bone grafts include autologous bone, allografts, and synthetic scaffolds [4]. Autologous bone is considered as the clinical gold standard due to its high efficacy of bone repair. However, this treatment is limited by both its supply and additional morbidities caused by bone harvesting. Allografts have a high failure rate in addition to a risk of disease transmission and quality inconsistency. Bone tissue engineering is an alternative approach that may be able to circumvent many of the above shortcomings [4,5].

Bone is a natural composite material consisting primarily of a collagen-containing organic polymer phase as a matrix and a mineral ceramic phase composed of hydroxyapatite [6]. Over the past decade, many efforts in bone tissue engineering have been dedicated to the development of biodegradable scaffolds with both excellent biocompatibility and mechanical properties mimicking those of natural bone tissues [7,8]. Many studies on ceramic/

* Corresponding author at: Department of Restorative Dentistry and Biomaterials, The University of Texas Health Science Center at Houston, Houston, TX, USA. Tel.: +1 713 500 4083; fax: +1 713 500 4372.
E-mail address: yunzhiyang@gmail.com (Y. Yang).

0014-3057/$ - see front matter © 2011 Elsevier Ltd. All rights reserved.
doi:10.1016/j.eurpolymj.2011.05.004

polymer composite scaffolds have attempted to take advantage of the strong compressive strength of ceramics as well as the flexibility of ductile polymers [9,10,2]. However, there has been only limited success in improving the mechanical strength of composite scaffolds through different methods, including the polymer matrix approach (top-down) [11,12] and the self-assembled mineralized collagen method (bottom-up) [13,14]. Coating is an alternative method for fabricating composite scaffolds by immersing polymer scaffolds into ceramic slurry [15,16], or coating the ceramic scaffolds with a thin layer of polymer [17,18]. For example, Miao et al. [19] found that the compressive strength of hydroxyapatite/β-tricalcium phosphate (HA/β-TCP) scaffolds prepared by a polyurethane foam replica method was significantly increased from 0.05 MPa before coating to 0.6 MPa after coating with poly(lactic-glycolic acid). Kim et al. [20] indicated that a polycaprolactone (PCL) coating on HA scaffolds improved the compressive strength of the HA scaffolds. The highest compressive strength obtained in PCL coated scaffolds was 0.45 MPa, which was approximately three times higher than that of the uncoated HA scaffold (0.16 MPa), but the compressive strength of the polymer coated ceramic composite scaffolds was still much lower than that of human cancellous bone (2–10 MPa) [21].

In our previous study, a novel method, named template-casting, was developed to produce a completely interconnected porous β-TCP scaffold with high compressive strength [22]. In this study, we aimed to develop a polymer/ceramic composite scaffold with enhanced bending strength and toughness by coating the ceramic scaffolds within a thin layer of polymer. Poly(lactic-co-glycolic acid) (PLGA) was used for it is an FDA-approved biodegradable polymer with ductility and excellent biocompatibility [23,24]. The open interconnected macropores of β-TCP scaffolds would allow for the infiltration of the polymer to homogeneously coat entire struts. This coating could achieve a highly interpenetrated polymer and ceramic network, potentially leading to a composite scaffold with higher mechanical strength and toughness. We first prepared PLGA coated β-TCP composite scaffolds, and then characterized the compressive strength, bending strength, and toughness of the scaffolds with and without the PLGA coating. Finally, we examined cell adhesion, proliferation, and differentiation on these scaffolds *in vitro*.

2. Materials and methods

2.1. Materials

β-Tricalcium phosphate powder with specific area of 17 m^2/g was purchased from Nanocerox Inc. (Ann Arbor, MI). Poly(lactic-glycolic acid) (PLGA, ratio M/M% 75:25, iv 0.2 dl/g) was purchased from PURAC America Co. Carboxymethyl cellulose (CMC) powders, paraffin granules, and anhydrous ethyl alcohol were purchased from Fisher Scientific (Pittsburgh, PA). All other chemicals were analytical grade and were used as received.

2.2. Preparation of β-TCP scaffold and PLGA-coated β-TCP composite scaffold

β-TCP scaffolds with completely interconnected pores were prepared by the template-casting method [22]. The method includes the preparation of paraffin spheres and β-TCP ceramic slurry, casting the slurry into a mold containing paraffin spheres, solidifying and sintering. Paraffin spheres were prepared by a conventional water-dispersion method [22]. The paraffin spheres with particle sizes between 0.71 and 1 mm were used in this study. β-TCP powder, CMC powder, dispersant (Darvan C) and surfactant (Surfonals) were mixed with distilled water while stirring to form the ceramic slurry. After filling the paraffin beads into customized molds, the β-TCP slurry was cast into the molds under a vacuum. The mold with slurry was dehydrated and solidified in a series of ethyl alcohol solutions, typically 70%, 90%, and 95% at 40–70 °C. After removing the dehydrated green body from the mold, the green body was put into an electric furnace and heated up to 1250 °C for 3 h to sinter the β-TCP scaffolds.

To fabricate the PLGA/β-TCP composite scaffolds, PLGA pellets were first dissolved in dichloromethane (CH_2Cl_2) solvent (10 wt%), then the β-TCP scaffolds were immersed into the PLGA solution under vacuum to allow for complete infiltration into the porous structures. The soaked scaffolds were then centrifuged at 300 rpm for 30 s to remove the excess PLGA solution from the scaffolds. The scaffolds were then taken out of the centrifuge tubes and left to dry in a fume hood overnight and dried again in an oven for 4 h at 45 °C, and further dried at least 3 days at room temperature to evaporate all of the organic solvent.

2.3. Characterizations

2.3.1. Porosity of the scaffolds before and after PLGA coating

To test the porosity of the β-TCP scaffolds with and without PLGA coating, a scaffold of weight W_s was immersed in a graduated cylinder containing a known volume (V_1) of water. The total volume of the water and scaffold was then recorded as V_2. The volume difference ($V_2 - V_1$) was the volume of the constructs of the scaffold. The bulk density (ρ_b) equals the weight of the scaffold (W_s) divided by the volume of the scaffold ($V_2 - V_1$). The theoretical density of β-TCP (ρ_t) is 3.156 g/cm^3 [22]. The porosity of scaffolds was determined by using the following equation: porosity = $(1 - \rho_b/\rho_t) \times 100\%$ [25]. The weight of each sample was measured using an electronic balance. At least three specimens were used to determine the porosity.

2.3.2. SEM analysis

A scanning electron microscope (FEI Quanta 400) was used for the morphological characterization of the scaffolds. The scaffolds were mounted onto aluminum stubs with double carbon tape and coated with gold using a sputter coater (CRC-150). The porous structure was observed under an acceleration voltage of 15 kV.

2.3.3. Mechanical testing

An Instron 4465 mechanical tester with a 5 KN load cell was used to test the compression strength and bending strength according to the guidelines of ASTM standards. The crosshead speed was set at 1 mm/min, and the load was applied until the scaffold cracked. The diameter of each sample was measured by a Vernier caliper before loading. For the compressive strength test, scaffold samples were polished on two opposite sides with sand paper using a metallic sample holder in order to ensure that the lower and upper sides were parallel. For the bending strength test, the span was kept at 20 mm. To calculate the bending strength of the scaffold, the following equation was used: $FL/\pi r^3$, where F represents the applied maximum load, L represents the span, and r represents the radius of the scaffold. Toughness, or energy absorption to failure, can be commonly determined by its absorption energy of mechanical deformation per unit volume (in unit of J/m^3). A toughness value was determined by integrating the area under the stress–strain curve from zero to the point of maximum stress for each individual specimen by Origin8.1 program (Originlab, USA) [26]. Three samples per group were measured, and each test repeated twice.

2.4. Biocompatibility in vitro

2.4.1. Cell culture and cell seeding

To evaluate the cell proliferation and differentiation on the scaffolds, rat bone marrow stromal cells (rBMSC) were separated from the gene-transferred rat by green fluorescent protein (GFP). The rBMSC were isolated from the femurs of rats and pooled to obtain a single cell suspension according to the instructions of a cell isolation kit (Chemicon International). Passage 5 rBMSC were used in this study, and the cells were grown in culture media containing Dulbecco's modified Eagle's medium (DMEM) supplemented with 10% FBS, 1% L-glutamine, 1% antibiotic–antimycotic solution and osteogenic factors (10 nM dexamethasone, 50 μg/mL L-ascorbic acid and 10 mM β-glycerophosphate). Medium was changed every 3 days. The scaffolds were decontaminated by soaking three times in 70% ethanol for 15 min each, and then rinsed three times with phosphate buffer solution (PBS) for 15 min before being left to dry overnight in a sterilized hood. Cells were loaded onto the sterilized scaffolds at a density of 1×10^5 cells/scaffold suspended in 100 μL culture media. The scaffolds used for the cell culture in this study were 8 mm in diameter and 6 mm in height. After 1 h incubation, the cell-seeded samples were cultured in 2 mL culture medium for the designated time points.

2.4.2. Cell morphologies

To investigate cell attachment ability and the cell morphologies on the scaffolds with and without PLGA coating, 1×10^5 cells were loaded on the scaffold and incubated in 2 mL culture medium. After day 3, the scaffolds were removed from the culture wells, rinsed with PBS (pH 7.4), and fixed with 4% paraformaldehyde in PBS for 1 h. The fixative was removed, and the wells were washed with PBS and the attached morphologies of rBMSCs grown on the β-TCP scaffolds were observed by a confocal laser scanning microscope (CLSM, Olympus IX81) after day 1 and 3 days. For SEM observation, fixed cells were washed and then post-fixed in 1% osmium tetroxide in PBS for 1 h followed by sequential dehydration in graded ethanol (70%, 90%, 95%, and 100%, each 10 min). The specimens were dried in hexamethyldisilizane (HMDS) for 5 min before sputter coating with gold for SEM analysis. The morphological characteristics of the attached cells on the scaffolds were observed using SEM (FEI Quanta 400).

2.4.3. MTT assay

3-(4,5-Dimethylthiazol-2-yl)-2,5-diphenyltetrasodium bromide (MTT) was used to quantify the number of metabolically active cells. At each time point (Day 1, 3, 5, 7), cells/scaffolds were transferred into a new 24-well plate and 1 mL of serum-free growth medium containing 100 μL 5 mg/mL MTT was added (1/10, final concentration was 0.5 mg/mL) into the 24 well plate. Cells were allowed to incubate at 37 °C for 4 h, during which time MTT was taken up by viable cells and reduced in the mitochondria to insoluble purple formazan granules. The formazan crystals formed were solubilized by adding 0.5 mL dimethyl sulfoxide for 30 min under shaking. The optical density (OD) of formazan in the solution was then read using a microplate reader at 490 nm (BIO-RAD Model 680). β-TCP scaffolds without PLGA coating were used as control.

2.5. Alkaline phosphatase activity

To evaluate alkaline phosphatase (ALP) activity, rBMSCs were seeded on the porous scaffolds for 1, 3, 7, 14, and 21 days. At each time point, cells were washed with PBS and lysed in 0.2% Triton X-100 solution for 30 min at room temperature after three freeze/thaw cycles (−80/37 °C). Cell lysates were placed in a 96-well plate for the measurement of ALP activity with *p*-nitrophenyl phosphate (*p*-NPP) substrate as described elsewhere [27]. The resultant absorbance values can be measured at 405 nm in a microplate reader (BIO-RAD Model 680, USA) after 30 min incubation at 37 °C. The amount of total protein in the cell lysates was determined using a micro-BCA Protein Assay Kit (Thermo Scientific). ALP activity was normalized to total protein concentration and expressed as units per gram of protein.

2.6. Statistical analysis

All the data were statistically analyzed using Student's *t* tests to investigate the significant difference between the two groups, before and after PLGA coating and are reported as mean values ± SD. Differences at a probability of less than 0.05 were considered to be statistically significant.

3. Results

3.1. Porous structures of β-TCP scaffolds with/without PLGA coating

In this study, a novel method, named template-casting, was used to prepare a porous β-TCP scaffold. By this

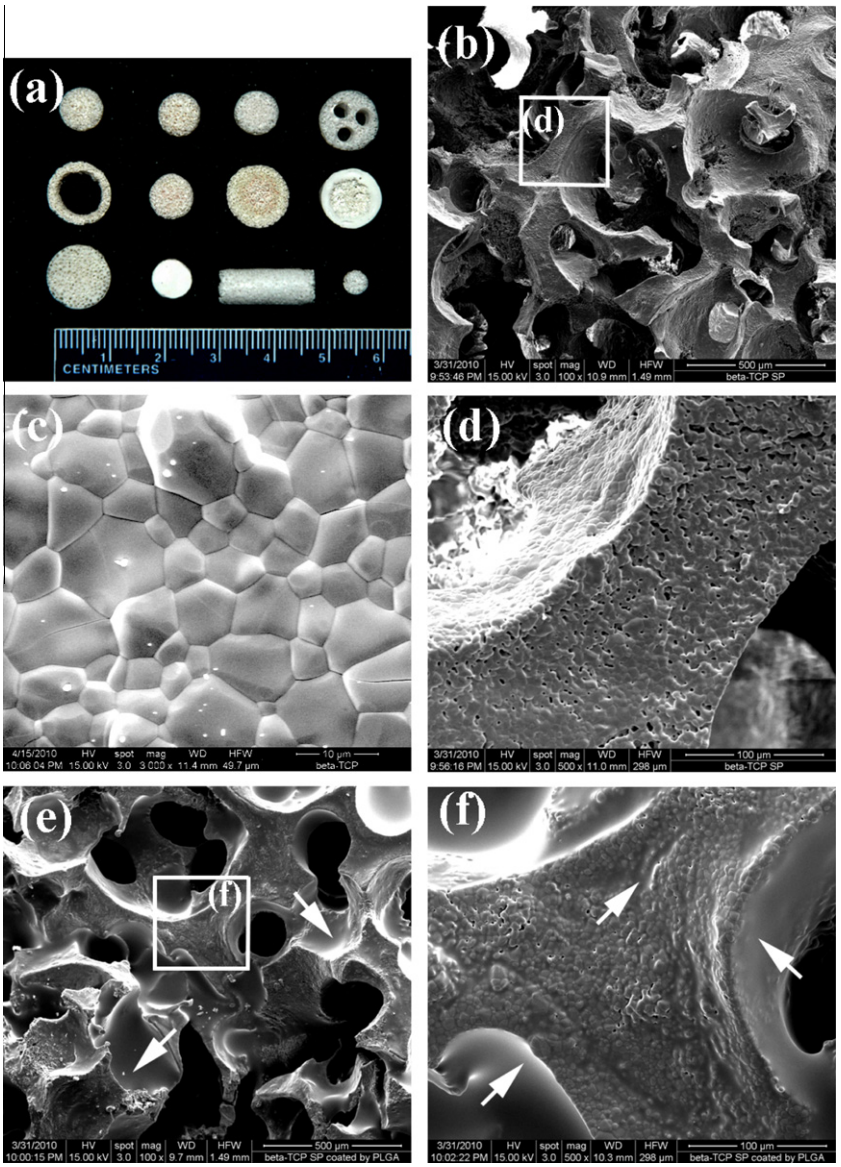

Fig. 1. Digital and SEM images of the scaffolds. (a) Scaffolds with different geometries. (b) The interconnected open macropores of the as-prepared scaffolds. (c) The β-TCP grains at a higher magnification. (d) The surface of the scaffold struts contains micropores. (e) The strut surface of the PLGA-coated β-TCP scaffolds after PLGA coating. (f) PLGA filled some open micropores in the struts. The white arrows indicate the PLGA coating and infiltration of PLGA into the micropores.

method, a β-TCP scaffold with completely interconnected macropores and high mechanical strength was successfully prepared. Fig. 1a demonstrates some scaffold examples of different geometries and shapes. Scaffolds with different geometries can be fabricated by customizing the templates in the designated shapes. Fig. 1b shows the interconnected open macropores of the as-prepared scaffolds, and the pore sizes range from 350 to 500 μm measured by NIH imageJ program. The β-TCP grains with sizes between 2 and 8 μm were measured using the NIH ImageJ program on the higher magnification SEM picture (Fig. 1c). The struts of the as-prepared scaffolds contain micropores (Fig. 1d). After the infiltration of PLGA solution followed by a drying process, the surfaces of the β-TCP scaffolds formed a thin PLGA layer (Fig. 1e), and some micropores in the struts became filled with PLGA (Fig. 1f), giving the surfaces a much smoother appearance compared to that of the uncoated struts (Fig. 1d). The thickness of the layer is less than 2 μm measured by ImageJ program. From the SEM observations, the thin coating of PLGA did not change the open macroporous structure when compared to the uncoated scaffold (Fig. 1b and e). The porosity of the β-TCP scaffold was 82.49 ± 0.04%, and decreased slightly after PLGA coating to 80.65 ± 0.02%, but there was no statistically significant difference as determined by *t*-test statistical analysis.

3.2. Mechanical properties of β-TCP and PLGA-coated β-TCP scaffolds

Fig. 2 indicates that the compressive strength of β-TCP scaffolds was 2.90 ± 0.67 MPa, while the compressive strength of PLGA-coated β-TCP scaffolds significantly increased to 4.19 ± 0.84 MPa. The compressive strength of the PLGA coated β-TCP scaffolds was significantly higher than that of the uncoated scaffolds. PLGA coating can penetrate some micropores and small cracks in the struts, resulting in increased compressive strength. However, overall compressive strength was mainly a result of the stiffness of the ceramic content. The strength of β-TCP scaffolds was reinforced by PLGA coating, and the compressive strength was comparable to that of cancellous bone (2–10 MPa) [18].

Fig. 3a shows typical load–displacement curves obtained in uniaxial tests performed on the β-TCP and PLGA-coated β-TCP scaffolds. The compression curves showed that β-TCP failed in an elastic-brittle manner, exhibiting a steep linear elastic region followed by a collapse plateau presumably dominated by brittle fracture of the struts. Some drops in load were observed from the curve, which could be associated with the development of microcracks in the struts of the scaffolds. The compression curve of PLGA-coated scaffold indicated the significant increase of this linear elastic region range followed by a steep drop and then a short plateau. This considerable yield resistance after coating is clearly superior to that of the plain β-TCP scaffold.

The bending strength of the scaffolds in the presence and absence of the PLGA coating was evaluated by a three-point bending test. Results demonstrated that the bending strength of the β-TCP scaffolds coated with PLGA was 40% higher than that of those without the PLGA polymer coating ($p < 0.05$). The bending strength increased from 1.46 ± 0.62 MPa for the uncoated scaffolds to 2.41 ± 0.45 MPa for the PLGA coated samples (Fig. 2).

Fig. 3b shows representative flexure load–deflection curves of experimental results obtained in the three-point bending test for the β-TCP scaffolds and PLGA-coated scaffolds. During the beginning stage, the two curves both had similar slopes, which demonstrated the linear elastic behavior of the scaffolds. However, plain β-TCP scaffolds broke at small stains, indicating the typical brittle behavior of ceramic, while the PLGA-coated scaffold resisted up to a 0.25 mm flexure deflection. An approximate eightfold increase in toughness of the PLGA-coated scaffolds (1.44 ± 0.95 MPa) was observed when compared to that of plain β-TCP scaffolds (0.17 ± 0.13 MPa) (Fig. 4a). The toughness of the coated scaffold significantly increased ($p < 0.01$). Despite cracking and breaking of the β-TCP struts early on, the broken parts were not separated and scattered, but remained an entire single piece held together by the PLGA. SEM observation showed that the PLGA formed a fibril-like structure bridging the crack opening as shown in Fig. 4b. With further displacement of the composite scaffold, the PLGA progressively began to reach its maximal crack opening and the entire piece of a composite scaffold separated.

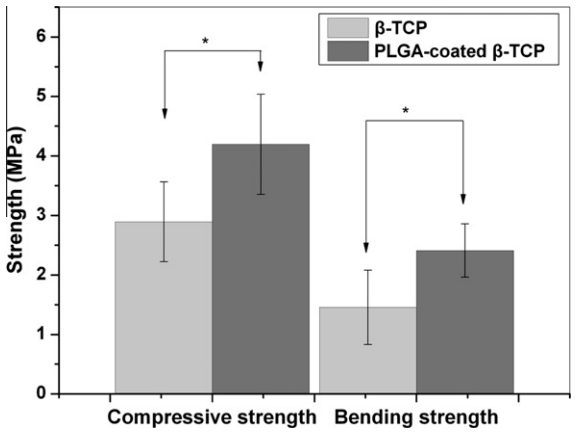

Fig. 2. The compressive and bending strength of the β-TCP and PLGA-coated β-TCP scaffolds. Marker indicates a significant difference ($p < 0.05$).

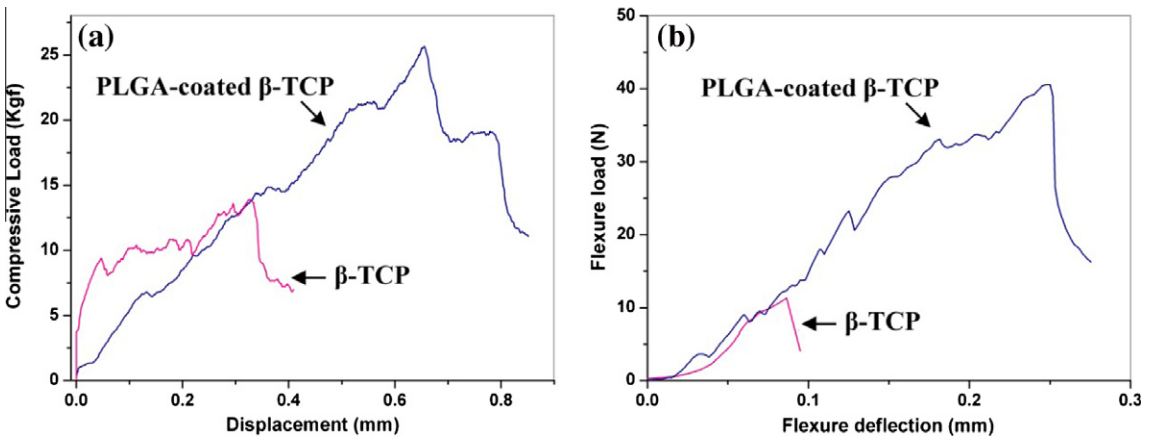

Fig. 3. Representative load–displacement curve obtained during uniaxial compression tests performed on the β-TCP and PLGA-coated β-TCP scaffolds (a). Representative flexure load–deflection curves obtained from three points bending tests performed on the β-TCP and PLGA-coated β-TCP scaffolds (b).

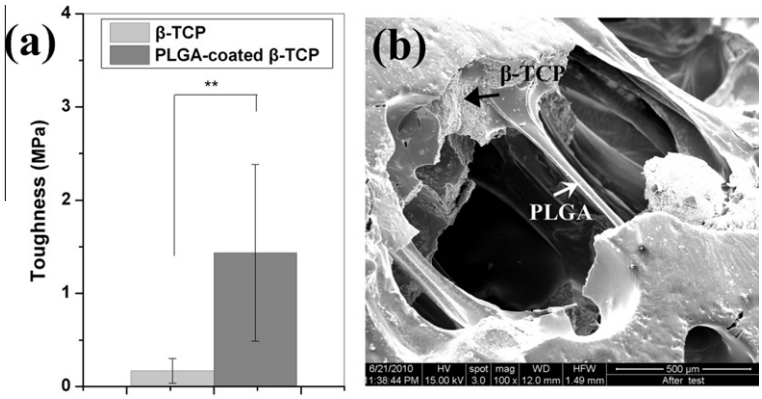

Fig. 4. (a) The toughness of the β-TCP and PLGA-coated β-TCP scaffolds, determined by area under the curves from flexure load–deflection curves ($p < 0.05$). (b) SEM micrograph of the fracture of the PLGA-coated during the bending test.

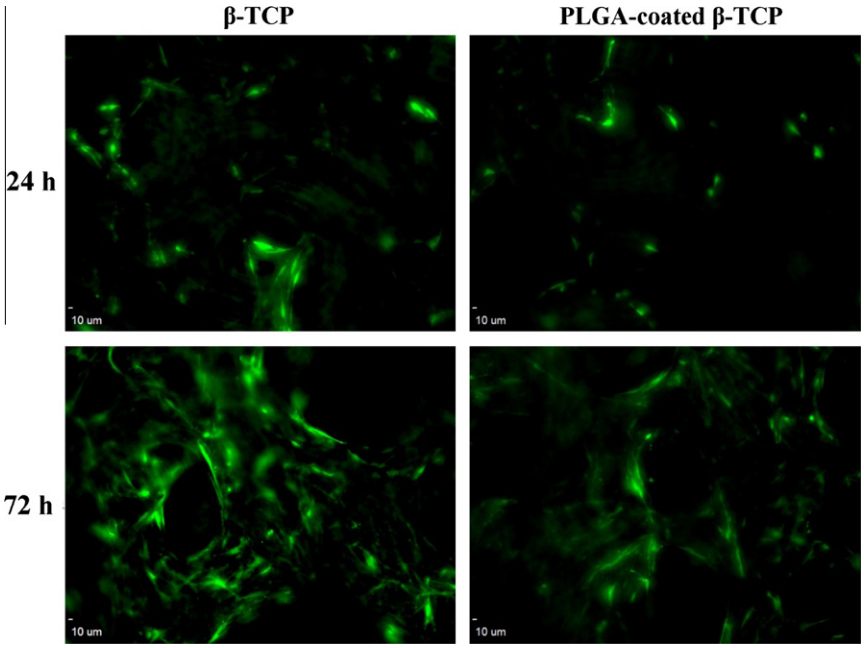

Fig. 5. Confocal laser scanning microscopy images of the morphology of rBMSCs on the β-TCP and PLGA-coated β-TCP scaffold after 24 and 72 h of incubation.

3.3. Cell attachment and morphologies

In order to observe the attachment of rBMSCs to the scaffold, a laser confocal fluorescent microscope was used to observe the morphologies of cells on the inner pores and struts of the scaffolds. It was seen that the cells attached well to the inner pore wall and strut surface of the β-TCP and the PLGA coating surface after seeding (Fig. 5). With incubation time, the cells continued to proliferate well on the β-TCP and the PLGA coated struts (Fig. 5). SEM images also indicate the adhesion and spreading of cells on the scaffolds (Fig. 6a and b). Together, these results suggest that cells can attach and spread well on the β-TCP and PLGA-coated composite scaffolds.

3.4. Biocompatibility of the scaffolds and cell proliferation

The MTT assay was used to determine the viability of cells grown on the scaffolds. Results showed that there was no significant difference in the optical density (OD) values between the β-TCP and PLGA-coated β-TCP scaffolds (Fig. 7). This result suggests that cells can proliferate well on both coated and uncoated β-TCP scaffolds.

3.5. Alkaline phosphatase activity

Alkaline phosphatase is one of the most widely recognized early biomarkers for bone progenitor cell differentiation. Alkaline phosphatase activity of rBMSC cells

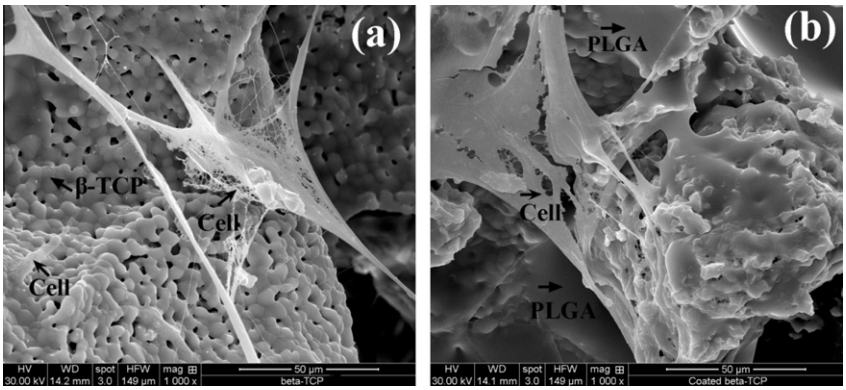

Fig. 6. SEM images of rBMSC on scaffolds. rBMSCs spread well on the β-TCP (a) and PLGA-coated β-TCP (b).

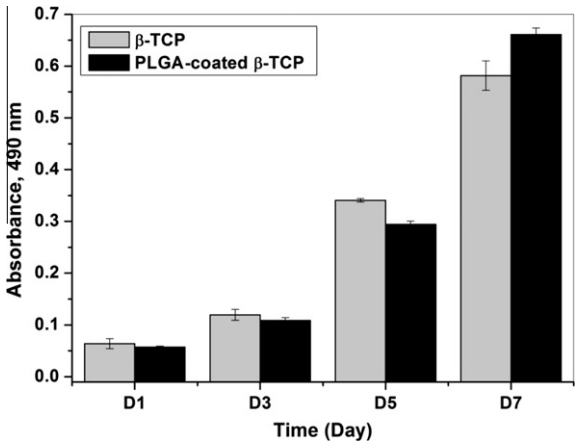

Fig. 7. Quantitative measurement of the amount of the formazan present in the cell seeded scaffolds by a MTT assay.

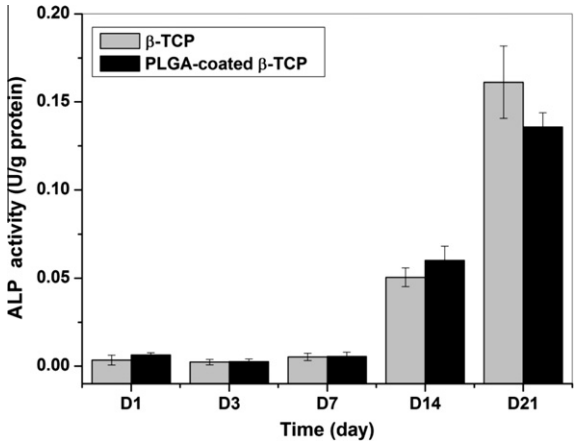

Fig. 8. Quantitative measurement of alkaline phosphatase activity in rBMSC cells on the β-TCP and PLGA-coated β-TCP scaffolds over time. There is no significant difference between the two groups ($p > 0.05$).

cultured on the β-TCP and PLGA-coated β-TCP scaffolds for 1, 3, 7, 14, and 21 days are presented in Fig. 8. Our results indicated that ALP activity on the β-TCP and PLGA-coated β-TCP composite scaffolds increased with culture time, and that there was no statistically significant difference between the two groups after *t*-test analysis. This result suggests that these cells were able to carry out osteogenic functions and differentiate on both the coated and uncoated β-TCP scaffolds.

4. Discussion

The scaffolds applied in bone regeneration should have an interconnected pore structure for new bone tissue ingrowth and have good mechanical properties to withstand loading during bone formation. β-TCP, a calcium phosphate (CaP) ceramic, has been used in clinics for bone repair due to its excellent osteoconductivity and biodegradability [28,29], but there is a great need to improve its toughness and reliability for use in load-bearing applications [28].

In our previous study, a template-casting method was developed to prepare β-TCP scaffolds with high compressive strength and completely interconnected pores. In this study, we hypothesized that a porous composite scaffold with high mechanical strength and toughness could be obtained through combining the template-casting and polymer impregnation methods. Our results manifested a 3D interconnected porous β-TCP/PLGA composite scaffold with significantly enhanced compressive strength, bending strength, and toughness. Coating with PLGA polymer resulted in the increase of the compressive strength of the scaffold from 2.90 to 4.19 MPa, bending strength from 1.46 to 2.41 MPa and toughness from 0.17 to 1.44 MPa. Clearly, the introduction of PLGA into porous β-TCP scaffolds effectively enhanced the mechanical properties of the β-TCP scaffold. It is worth noting that the significant increase in mechanical strength of the composite scaffolds was primarily not a result of the decrease in porosity, though the decrease in porosity by approximately 2% would lead to the slight increase of compressive strength of scaffolds [28]. The porosity reduction in our study was consistent with Chen's study [30], in which there was

about 2.2% reduction in macroporosity after the polymer coating on the ceramic scaffolds. Since the pores of the β-TCP scaffold prepared by the template-casting were large and completely interconnected, the infiltration of polymer formed a continuous and interconnected coating on the β-TCP scaffold. This thin layer of polymer leads to the systemic coating of all the struts and the formation of the highly organized and interpenetrating polymer/ceramic composite at the strut level. This interpenetrating structural characteristic is probably responsible for the strengthening and toughening of the composite scaffolds. In general, a ceramic scaffold has open micropores and defects such as microcracks in the struts after sintering. The infiltration of a polymer filled pre-existing open micropores and exposed microcracks on the surface of scaffolds and formed an interlaced structure. This interlaced and continuous layer of polymer further inhibited the propagation of cracks in the ceramic. This defect healing mechanism has already been described in Pedro Miranda's study about the mechanism of strengthen in β-TCP rods [31]. From the load–displace curve of the β-TCP/PLGA composite scaffolds in Fig. 3, the observation of a significant increase of linear elastic region range before a steep drop and then a small plateau clearly demonstrated that there was a considerable yield resistance increase after coating. In the present study, the observation of stretched fibrils in the fracture surface (Fig. 4b) also suggested another toughening mechanism: crack bridging. According to Pezzotti and Asmus [32], when microcracks propagate, the ductile polymer ligaments could be stretched upon crack opening and consume energy. The toughness of bone tissue is partially due to crack bridging by collagen fibrils [17,33]. In other words, the PLGA appeared to act like natural collagen fibrils, enhancing the toughness of the PLGA-coated β-TCP scaffolds by a similar mechanism (Fig. 4). Therefore, the combination of the systematic coating of struts, the interpenetrating structural characteristics, and crack bridging significantly improved the mechanical strength of the composite scaffolds and enhanced their toughness. In the future, we may also further improve the mechanical strength and toughness of composite scaffolds for load-bearing applications by optimizing the structural design, polymer/ceramic combinations, polymer infiltration process, and interface interaction between polymer and ceramic.

In this study, we investigated the biocompatibility of the composite scaffolds by performing cell attachment, proliferation, and differentiation assays. Our results indicated that rBMSC cells seeded on both the scaffolds were able to proliferate and differentiate. No significant difference in cell behavior was observed, suggesting that both the polymer coated scaffolds and uncoated scaffolds exhibited excellent biocompatibility. Additionally, the bioactivity of composite scaffolds can be further enhanced by incorporating bioactive macromolecules, such as cytokines or growth factors, or mixing some bioactive phase, such as inorganic powders, into the polymer coating [34]. This polymer coating can function as a carrier for the controlled release of biological cues to guide cell response in addition to strengthening and toughening the composite scaffolds for the repair of large bone defects.

5. Conclusions

Here we show that a combination of template-casting and polymer impregnation methods can be used to fabricate a completely interconnected porous ceramic/polymer biodegradable scaffold with significantly improved mechanical performance and excellent biocompatibility. The enhancement of the composite scaffold's characteristics is due to a combination of the systematic coating of struts, the interpenetrating structural characteristics, and the crack bridging by the polymer. The structural gradation, interconnected pore sizes and porosity of these composite scaffolds can easily be regulated. The infiltrated polymer coating can also be used for the controlled release of biological cues.

Acknowledgments

We would like to acknowledge the supports in part by research Grant No. 1-FY06-918 from the March of Dimes Birth Defect Foundation, Airlift Research Foundation, Wallace H. Coulter Foundation, DOD W81XWH-10-1-0966, NIH R01AR057837 from NIAMS, and NIH R01DE021468 from NIDCR. We thank Dr. Shiwei Cai for providing rBMSC cells for the cell experiments.

References

[1] Vacanti CA, Kim W, Upton J, Vacanti MP, Mooney D, Schloo B, et al. Tissue-engineered growth of bone and cartilage. Transplant Proc 1993;25:1019–21.
[2] Kim SS, Sun Park M, Jeon O, Yong Choi C, Kim BS. Poly(lactide-co-glycolide)/hydroxyapatite composite scaffolds for bone tissue engineering. Biomaterials 2006;27(8):1399–409.
[3] Donati D, Zolezzi C, Tomba P, Viganò A. Bone grafting: historical and conceptual review, starting with an old manuscript by Vittorio Putti. Acta Orthop 2007;78(1):19–25.
[4] Mikos AG, Herring SW, Ochareon P, Elisseeff J, Lu HH, Schoen FJ, et al. Engineering complex tissues. Tissue Eng 2006;12(12):3307–39.
[5] Gupta AP, Kumar V. New emerging trends in synthetic biodegradable polymers – polylactide: a critique. Eur Polym J 2007;43:4053–74.
[6] Rho JY, Kuhn-Spearing L, Zioupos P. Mechanical properties and the hierarchical structure of bone. Med Eng Phys 1998;20(2):92–102.
[7] Holland TA, Mikos AG. Review: biodegradable polymeric scaffolds. Improvements in bone tissue engineering through controlled drug delivery. Adv Biochem Eng Biot 2006;102:161–85.
[8] Zhang R, Ma PX. Poly(α-hydroxyl acids)/hydroxyapatite porous composites for bone–tissue engineering. I. Preparation and morphology. J Biomed Mater Res 1999;44:446–55.
[9] Navarro M, Ginebra MP, Planell JA, Zeppetelli S, Ambrosio L. Development and cell response of a new biodegradable composite scaffold for guided bone regeneration. J Mater Sci: Mater Med 2004;15:419–22.
[10] Rezwan K, Chen QZ, Blaker JJ, Boccaccini AR. Biodegradable and bioactive porous polymer/inorganic composite scaffolds for bone tissue engineering. Biomaterials 2006;27(18):3413–31.
[11] Torres FG, Nazhat SN, Sheikh SH, Fadzullah Md, Maquet V, Boccaccini AR. Mechanical properties and bioactivity of porous PLGA/TiO_2 nanoparticle-filled composites for tissue engineering scaffolds. Compos Sci Technol 2007;67:1139–47.
[12] Fabbri P, Cannillo V, Sola A, Dorigato A, Chiellini F. Highly porous polycaprolactone-45S5 Bioglass® scaffolds for bone tissue engineering. Compos Sci Technol 2010;70:1869–78.
[13] Cui FZ, Li Y, Ge J. Self-assembly of mineralized collagen composites. Mater Sci Eng R 2007;R57:1–27.
[14] Hosseinkhania H, Hosseinkhanib M, Tianc F, Kobayashic H, Tabata Y. Ectopic bone formation in collagen sponge self-assembled peptide–amphiphile nanofibers hybrid scaffold in a perfusion culture bioreactor. Biomaterials 2006;27:5089–98.
[15] Roether JA, Boccaccini AR, Hench LL, Maquet V, Gautier S, Jerome R. Development and in vitro characterisation of novel bioresorbable

and bioactive composite materials based on polylactide foams and Bioglass® for tissue engineering applications. Biomaterials 2002;23:3871–8.
[16] Verheyen CCPM, de Wijn JR, van Blitterswijk CA, de Groot K, Rozing PM. Hydroxyapatite/poly(L-lactide) composites: an animal study on push-out strengths and interface histology. J Biomed Mater Res 1993;27:433–44.
[17] Peroglio M, Gremillard L, Chevalier J, Chazeau L, Gauthier C, Hamaide T. Toughening of bio-ceramics scaffolds by polymer coating. J Eur Ceram Soc 2007;27:2679–85.
[18] Zhao J, Lu X, Duan K, Guo LY, Zhou SB, Weng J. Improving mechanical and biological properties of macroporous HA scaffolds through composite coatings. Colloid Surface B 2009;74:159–66.
[19] Miao XG, Tan MF, Li J, Xiao Y, Crawford R. Mechanical and biological properties of hydroxyapatite/tricalcium phosphate scaffolds coated with poly(lactic-co-glycolic acid). Acta Biomater 2008;4:638–45.
[20] Kim HW, Knowles JC, Kim HE. Hydroxyapatite/poly(e-caprolactone) composite coatings on hydroxyapatite porous bone scaffold for drug delivery. Biomaterials 2004;25:1279–87.
[21] Gibson LG. The mechanical behavior of cancellous bone. J Biomech 1985;18:317–28.
[22] Liu YX, Kim JH, Young D, Kim SW, Nishimoto SK, Yang YZ. Novel template-casting technique for fabricating b-tricalcium phosphate scaffolds with high interconnectivity and mechanical strength and in vitro cell responses. J Biomed Mater Res 2010;92A:997–1006.
[23] Chastain SR, Kundu AK, Dhar S, Calvert JW, Putnam AJ. Adhesion of mesenchymal stem cells to polymer scaffolds occurs via distinct ECM ligands and controls their osteogenic differentiation. J Biomed Mater Res 2006;78A(1):73–85.
[24] Mao JJ, Xin X, Hussain M. Continuing differentiation of human mesenchymal stem cells and induced chondrogenic and osteogenic lineages in electrospun PLGA nanofiber scaffold. Biomaterials 2007;28(2):316–25.
[25] Karageorgiou V, Kaplan D. Porosity of 3D biomaterial scaffolds and osteogenesis. Biomaterials 2005;26:5474–91.
[26] Porter NL, Pilliar RM, Grynpas MD. Fabrication of porous calcium polyphosphate implants by solid freeform fabrication: a study of processing parameters and in vitro degradation characteristics. J Biomed Mater Res 2001;56(4):504–15.
[27] Hutmacher DW, Schantz JT, Lam CXF, Tan KC, Lim TC. State of the art and future directions of scaffold-based bone engineering from a biomaterials perspective. J Tissue Eng Regen Med 2007;1:245–60.
[28] Wagoner Johnson AJ, Herschler BA. A review of the mechanical behavior of CaP and CaP/polymer composites for applications in bone replacement and repair. Acta Biomater 2011;7(1):16–30.
[29] Rezwan K, Chen Q, Blaker J, Boccaccini A. Biodegradable and bioactive porous polymer/inorganic composite scaffolds for bone tissue engineering. Biomaterials 2006;27:3413–31.
[30] Chen QZ, Boccaccini AR. Poly(D, L-lactic acid) coated 45S5 bioglass-based scaffolds: processing and characterization. J Biomed Mater Res A 2006;77A:445–57.
[31] Martínez-Vázquez FJ, Perera FH, Miranda P, Pajares A, Guiberteau F. Improving the compressive strength of bioceramic robocast scaffolds by polymer infiltration. Acta Biomater 2010;6(11):4361–8.
[32] Pezzotti G, Asmus SMF. Fracture behavior of hydroxyapatite/polymer interpenetrating network composites prepared by in situ polymerization process. Mater Sci Eng A (Struct Mater:Prop, Microstruct Process) 2001;A316:231–7.
[33] Nalla RK, Kinney JH, Ritchie RO. Mechanical fracture criteria for the failure of human cortical bone. Nat Mater 2003;2:164–8.
[34] Roohani-Esfahani SI, Nouri-Khorasani S, Lu Z, Appleyard R, Zreiqat H. The influence hydroxyapatite nanoparticle shape and size on the properties of biphasic calcium phosphate scaffolds coated with hydroxyapatite-PCL composites. Biomaterials 2010;31(21):5498–509.